ELSEVIER

Journal of Nuclear Materials 305 (2002) 169–174

journal of nuclear materials

www.elsevier.com/locate/jnucmat

Characterisation of microstructural parameters in oxygen-irradiated Zr–1.0%Nb–1.0%Sn–0.1%Fe

P. Mukherjee [a,*], P. Barat [a], S.K. Bandyopadhyay [a], P. Sen [a], S.K. Chottopadhyay [b], S.K. Chatterjee [b], M.K. Mitra [c]

[a] *Variable Energy Cyclotron Centre, 1/AF Bidhannagar, Kolkata 700 064, India*
[b] *Regional Engineering College, Durgapur 713 209, India*
[c] *Department of Metallurgy, Jadavpur University, Kolkata 700 032, India*

Received 9 April 2002; accepted 14 June 2002

Abstract

We have characterised the microstructural parameters like domain size, microstrain within the domain, dislocation density and stacking fault probabilities in Zr–1.0%Nb–1.0%Sn–0.1%Fe alloy, irradiated with 116 MeV O^{5+} ion at different doses, by X-ray diffraction line profile analysis using modified Rietveld technique. The analysis revealed that there is a significant decrease in domain size but increase in microstrain and dislocation density with dose of irradiation. These microstructural parameters have been compared with our earlier observations on the same alloy irradiated at different doses with 15 MeV proton. We find significant changes of these parameters in oxygen-irradiated samples as compared to the proton-irradiated samples. The variations of microstructures in these samples have been explained in the light of the mechanism of defect evolution for light and heavy ion irradiation.

PACS: 6160; 6170.A; 6180.F

1. Introduction

Materials irradiated with energetic particles respond by undergoing changes in structure and properties. Energetic particles transfer energy to the materials primarily by the process of ionisation, electronic excitation and also by displacements of atoms from their original sites. These cause a change in the internal microstructures, phase distributions, dimensions, mechanical and corrosion properties [1–5]. Heavy ions in the MeV energy range impart energy to the atoms of the target materials and produce a displacement cascade consisting of highly localized interstitials and vacancies [6]. In case of light ions such as protons, the damage profiles are much more homogeneous than for heavy ions. Keeping the technological interests in view, several studies have been done on the problems of simulating fission and fusion neutron damage with light and heavy ions [7–11]. Extensive studies have also been carried out on the nuclear structural materials [12,13] on the response of light and heavy particle irradiation and consequent defect production and microstructural evolution. The nature of radiation damage in these materials is affected by the type of ions, alloying elements and impurity variations [14]. In our earlier studies [15,16], we have seen that irradiation of new zirconium alloy (Zr–1.0%Nb–1.0%Sn–0.1%Fe) of thickness 0.4 mm with 15 MeV proton resulted in di- and tri-vacancy clustering. However, the dislocation density of the unirradiated and irradiated samples remained unchanged.

In the present work, we have carried out the irradiation with 116 MeV O^{5+} ion on the same zirconium based alloy of 0.4 mm thickness at different doses. We

* Corresponding author. Tel.: +91-33 337 1230; fax: +91-33 334 6871.
E-mail address: paramita@veccal.ernet.in (P. Mukherjee).

0022-3115/02/$ - see front matter
PII: S0022-3115(02)00933-9

have characterised the domain size, microstrain, dislocation density and stacking fault probabilities of the unirradiated and irradiated alloy by X-ray diffraction line profile analysis (XRDLPA) using modified Rietveld technique [17]. The damage profile as a function of depth from the surface has been characterised in terms of displacements per atom (dpa) for different doses. The idea of this work is to compare the variation of microstructural parameters in new zirconium alloy caused by heavy and light ion (proton) irradiation.

2. Experimental

Ingot of new zirconium alloy was prepared in Nuclear Fuel Complex, Hyderabad, India, by double vacuum arc melting technique. It was then β quenched, followed by hot extrusion and cold pilgering for producing fuel cladding tubes of 0.4 mm wall thickness.

Samples of size 10 mm × 10 mm were cut from these tubes and annealed at a temperature of 1023 K for 4 h. The samples were mounted on an aluminium flange and then irradiated with 116 MeV O^{5+} ions from Variable Energy Cyclotron (VECC), Kolkata, India. The irradiation doses were 1×10^{17}, 5×10^{17}, 1×10^{18} and 5×10^{18} O^{5+} ions/m^2. The flange used in irradiation was cooled by continuous flow of water. During irradiation, the temperature of the sample did not rise above 313 K as measured by the thermocouple connected with the closest proximity of the sample. The dpa was obtained by Monte-Carlo simulation technique using the code SRIM 2000 [18].

X-ray diffraction profiles for each irradiated sample have been recorded using Philips 1710 X-ray diffractometer using Cu Kα radiation. The 2θ ranging from 25° to 100° with a step scan of 0.02° was used. The time per step was 4 s.

3. Method of analysis

X-ray data were analysed for domain size and root mean squared strain with the help of modified Rietveld technique using the program LS1 [17].

The program LS1 includes the simultaneous refinement of crystal structure and microstructural parameters like domain size and microstrain within the domain. The method involves the Fourier analysis of the broadened peaks [17]. The initial values of the lattice parameters were obtained from a least square fit of the powder diffraction peaks. The XRD patterns revealed a primary phase α. The β phase which is present in the alloy [19], in a very small fraction could not be detected by XRD. The lattice parameters, average domain size (D_{av}) and microstrain $\langle \varepsilon_l^2 \rangle^{1/2}$ were used as fitting parameters simultaneously to obtain the best fit in order to calculate the average values of the fitting parameters. The effective domain size (D_e) with respect to fault-affected crystallographic planes was then refined to obtain the best fitting parameters. The X-ray diffraction peak profiles have been described by the pseudo-Voigt function [17] for the unirradiated and irradiated samples in order to fit the experimental data. The orientation parameters were also used as a fitting parameters [20–22] to incorporate the corrections for the preferred orientation as Zirconium and its alloys show strong crystallographic texture along certain crystallographic direction after mechanical working [23]. The instrumental broadening correction was done by a silicon sample which has large crystallites and is free from any defect.

The dislocation densities ρ have been measured from the relation [24] $\rho = (\rho_D \rho_S)^{1/2}$, where $\rho_D = 3/D_{av}^2$ (dislocation density due to domain size) and $\rho_S = k\langle \varepsilon_l^2 \rangle / \bar{b}^2$ (dislocation density due to strain), k is a material constant and $\bar{b}$ is the modulus of Burger's vector, $\frac{1}{3}[1\,1\,\bar{2}\,0]$.

The effective domain size is related to the average domain size and the stacking faults (deformation fault α and growth fault β) by the following relations [25]:

$$\frac{1}{D_e} = \frac{1}{D_{av}} + \left[|L_0| d(3\alpha + 3\beta)/C^2 \right] \quad (1)$$

for L_0 even in case of HKL_0 reflection.

$$\frac{1}{D_e} = \frac{1}{D_{av}} + \left[|L_0| d(3\alpha + \beta)/C^2 \right] \quad (2)$$

for L_0 odd in case of HKL_0 reflection, where d is the lattice spacing and C is the lattice constant. The deformation fault α and growth fault β were then separated by least square analysis considering the fault affected reflections.

4. Results and discussion

Fig. 1 represents the typical X-ray diffraction profile of the sample irradiated with 5×10^{17} O^{5+} ions/m^2 dose of oxygen ions. There is a clear indication of peak broadening in the diffraction profiles of the irradiated samples as compared to the un-irradiated ones. The broadening of the peaks has resulted from the irradiation induced defects. There is no major phase change occurred during oxygen irradiation as we did not observe any additional peak in the X-ray diffraction profiles of the irradiated samples. The microstructural parameters of the oxygen-irradiated samples at doses 1×10^{17}, 5×10^{17}, 1×10^{18} and 5×10^{18} O^{5+} ions/m^2 have been characterised by XRDLPA using modified Rietveld technique [17]. The best fit values of the domain size and microstrain for un-irradiated and oxygen-irradiated samples have been plotted against the dose and are shown in Figs. 2 and 3, respectively.

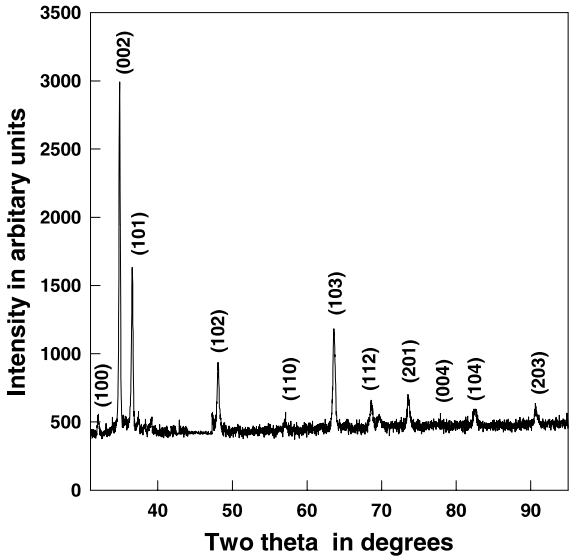

Fig. 1. XRD pattern for sample irradiated with 5×10^{17} O^{5+} m^{-2}.

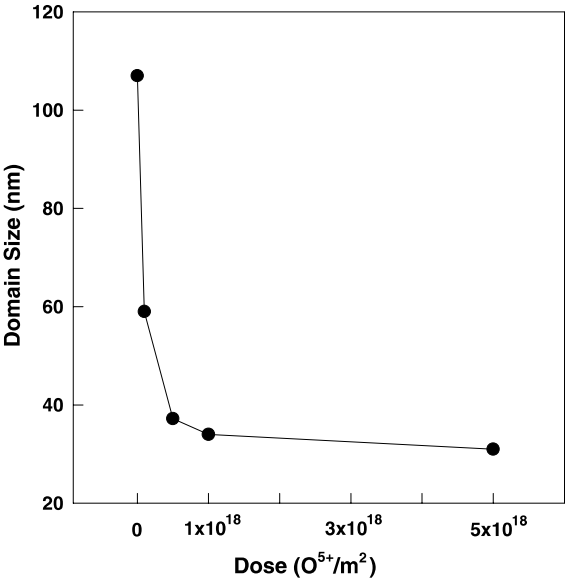

Fig. 2. Variation of domain size with dose.

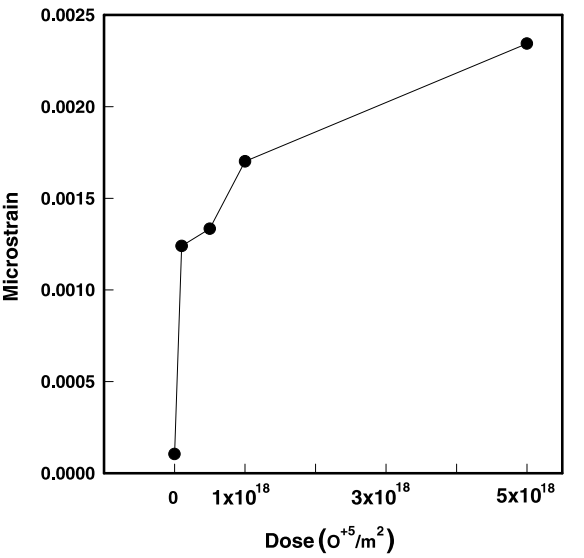

Fig. 3. Variation of microstrain with dose.

In our earlier observations [15,16] on Zr–1.0%Nb–1.0%Sn–0.1%Fe samples irradiated with proton of 15 MeV, we have seen by positron annihilation spectroscopy studies that there was a generation of irradiation-induced di- and tri-vacancy clusters. But there was no broadening of the diffraction peaks. The domain size and the microstrain values did not change significantly. The order of dislocation density also remained almost unchanged even up to the highest dose of irradiation [16], as seen by XRDLPA. We further concluded that proton irradiation at these doses on Zr–1.0%Nb–1.0%Sn–0.1%Fe samples did not generate additional dislocation loops through collapse of point defects.

On the contrary, we find significant changes in the domain size, microstrain and dislocation density with dose in oxygen-irradiated samples as compared to the un-irradiated sample as observed in Figs. 2–4, respectively. There is a drastic decrease in domain size from un-irradiated samples to the samples at a dose of 5×10^{17} O^{5+} m^{-2} but these values saturate with increasing dose of irradiation. The values of microstrain are found to increase with dose. The dislocation density increases almost by an order of magnitude for the samples irradiated with 1×10^{18} and 5×10^{18} O^{5+} m^{-2} as compared to the un-irradiated samples. These values are also found to saturate with dose (Fig. 4). The dislocation density was found to be $\sim 10^{15}$ m^{-2} for the samples irradiated with 5×10^{17}, 1×10^{18} and 5×10^{18} O^{5+} ions/m^2. The reasons of the above findings can be explained as follows.

The range of 15 MeV proton in the alloy obtained by SRIM 2000 calculation was found to be 720 μm which is more than the thickness of the samples (400 μm). Hence, the proton completely penetrated the sample and only partial energy of the proton beam was deposited on it. The damage produced in the samples was a bulk phenomenon due to complete penetration of the proton beam. On the contrary, the range of 116 MeV O^{5+} beam in the alloy is around 67 μm as calculated by SRIM 2000. Oxygen being a heavy ion impart so much energy to the primary knock on atoms that a displacement cascade is produced consisting of highly localized production of interstitials and vacancies associated with a

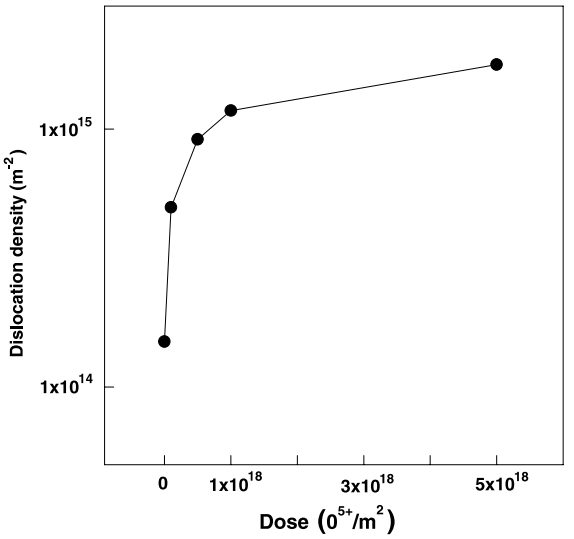

Fig. 4. Variation of dislocation density with dose.

single initiated event. This phenomenon is not observed in the samples irradiated with proton which is a light charged particle and we see [15,16] that agglomeration of vacancies was restricted up to tri-vacancy clustering.

The reaction pathways of proton beam through the sample of 400 μm thickness produces fairly uniform radiation damage. Moreover, the damage energy deposition with distance i.e. dE/dx is found to be almost two orders less than that of oxygen beam as shown in Fig. 5 (calculated from the code SRIM 2000 [18]). On the other hand, oxygen beam is stopped within 67 μm and the energy transferred to lattice atoms are much larger at

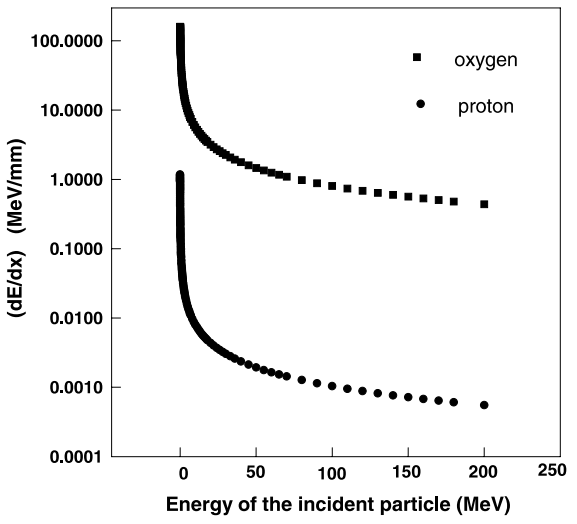

Fig. 5. Variation of (dE/dx) with respect to energy of the incident particle (MeV).

the end. Besides, as the primary recoil proceeds through the sample, loosing energy in successive collisions, the displacement cross-section increases [26]. Thus the distance between successive displacements decreases [26] and at the end of its track, the recoil collides with practically every atom in its path, creating a very high local concentration of vacancies and interstitials. Thus, a concentration gradient of defects within a small reaction path (67 μm) is present in the samples for the damage associated with oxygen beam. This gradient helps in migration of defects within a short distance and also agglomeration of them. The accumulation of defects causes the nucleation of defect clusters, which collapses in the shape of dislocation loops [27]. As a result, we find a significant change in dislocation density in the irradiated samples than unirradiated samples as shown in Fig. 4. This is not expected for the damage produced by proton beam where the concentration of defects is less throughout its path length.

The radiation damage which is generally assayed by the damage energy deposition causing displacements of atoms for the highest dose sample is found to be 4.38×10^{-3} dpa for proton-irradiated samples with highest dose (5×10^{21} protons m^{-2}) and 4.30×10^{-3} dpa for oxygen-irradiated samples with highest dose (as calculated from the code SRIM 2000 [18]). Therefore, it is interesting to note that the microstructural parameters are quite different in the samples irradiated with heavy ions and light ions though the equivalent dpa are obtained in both the cases.

The domain sizes of the irradiated samples decrease due to the formation of dislocation substructures, which have resulted due to the entanglement of dislocations among themselves by the interactions of stress fields around them. The decrease in domain size is quite drastic at the lower doses but almost saturates with higher doses as the generation of dislocations did not vary significantly at higher doses.

The compound fault parameters $(3\alpha + 3\beta)$ when L_0 is even and $(3\alpha + \beta)$ when L_0 is odd are shown in Table 1. The deformation fault α and growth fault β calculated from the compound fault values for various reflections at all doses are also shown in Table 1.

The values of α and β are found to be negligibly small for unirradiated and irradiated samples at all doses of irradiation. This observation tends to confirm that the deformation and growth fault are almost absent in these alloy systems [28] and the faulting probability of this alloy did not change significantly even after irradiation with oxygen ion. The stacking fault energy for zirconium base alloys is very high [29], which is not affected by the irradiation induced defect up to the experimental limit of irradiation dose. The absence of growth faults in these alloy systems is exactly like other hexagonal alloy systems [28–31]. This observation corroborates also with the similar observations obtained from pure zirconium

Table 1
The effective domain size (D_e) and compound fault parameters for unirradiated and samples irradiated with oxygen

Sample (O^{5+} m^{-2})	Fault-affected reflections	Effective domain size, D_e (nm)	Compound fault parameters (10^{-3})		Fault densities (10^{-3})	
			L_0 = even ($3\alpha + 3\beta$)	L_0 = odd ($3\alpha + \beta$)	α	β
Unirradiated	102	109	−0.13		−0.02	−0.01
	202	106	0.03			
	104	112	−0.25			
	101	106		0.03		
	103	111		−0.20		
	203	108		−0.07		
1×10^{17}	102	52	1.68			
	202	43	5.86			
	104	67	0.20			
	101	45		5.86	0.73	−0.2
	103	56		0.60		
	203	49		2.89		
5×10^{17}	102	33	2.20			
	202	30	6.85			
	104	36	0.60			
	101	30		6.90	1.44	−7.63
	103	35		1.50		
	203	32		3.50		
1×10^{18}	102	32	1.80			
	202	29	6.30			
	104	35	1.50			
	101	29		6.30	6.59	−2.0
	103	34		4.60		
	203	30		3.20		
5×10^{18}	102	28	2.70			
	202	27	5.59			
	104	28	2.33			
	101	27		5.63	6.8	−1.21
	103	28		2.30		
	203	28		3.50		

[30] where α was found to be $\sim 4.5 \times 10^{-3}$ and also for heavily cold-worked zirconium base alloys obtained by Warren–Averbach technique [32].

5. Conclusions

The microstructural parameters of Zr–1.0%Nb–1.0%Sn–0.1%Fe alloy irradiated with 116 MeV O^{5+} have been reliably assessed through the XRDLPA using modified Rietveld Technique. The analysis revealed that there is a significant decrease in the domain size but an increase in microstrain values. The damage associated with oxygen beam is quite extensive and produces highly localised concentrations of defects. The accumulation of defects causes the nucleation of defect clusters, which collapses in the shape of dislocation loops and the density of dislocations increases accordingly. This phenomenon is not observed with proton-irradiated samples with almost equivalent dpa and the agglomeration of defects was restricted upto tri-vacancy clustering only. The stacking fault probability of this alloy did not change significantly even after irradiation with oxygen ion.

References

[1] Y. Adda, in: J. Corbett, L.C. Ianniello (Eds.), Radiation Induced Voids in Metals, Albany, 9–11 June, p. 30.
[2] R.L. Fleischer, Acta Metall. 10 (1962) 840.
[3] H.R. Higgy, F.H. Hammad, J. Nucl. Mater. 55 (1975) 177.
[4] G.S. Was, S.M. Bruemmer, J. Nucl. Mater. 216 (1994) 326.
[5] L.K. Mansur, J. Nucl. Mater. 216 (1994) 97.
[6] C. Abromeit, J. Nucl. Mater. 216 (1994) 78.
[7] J.O. Stiegler (Ed.), Workshop on Correlation of Neutron and Charged Particle Damage, Oak Ridge, 1976, conf-760673.

[8] M.L. Bleiberg, J.W Bennet (Eds.), International Conference on Radiation Effects in Breeder Reactor Structural Materials, Scottsdale, 1977.
[9] H.R. Brager, J.S. Perrin (Eds.), International Conference On Effects of Radiation on Materials, Scottsdale, ASTM, Philadelphia, PA, 1982.
[10] F.A. Garner, N.H. Packan, A.S. Kumar, International Conference on Radiation-induced Changes in Microstructure, Seattle, ASTM, Philadelphia, PA, 1986.
[11] G. Scenes (Ed.), International Conference on Physics of Radiation Effects in Metals, Siofok 1991, Mater. Sci. Forum, 1992, p. 97.
[12] Y. Etoh, S. Shimada, J. Nucl. Mater. 200 (1993) 59.
[13] P. Merle, K. Loucif, L. Adami, R. Borrelly, J. Nucl. Mater. 159 (1988) 149.
[14] M. Griffiths, J. Nucl. Mater. 159 (1988) 190.
[15] P. Mukherjee, P.M.G. Nambissan, P. Sen, P. Barat, S.K. Bandyopadhyay, J. Nucl. Mater. 273 (1999) 338.
[16] P. Mukherjee, P.M.G. Nambissan, P. Sen, P. Barat, S.K. Bandyopadhyay, J.K. Chakravartty, S.L. Wadekar, S. Banerjee, S.K. Chattopadhyay, S.K. Chatterjee, M.K. Mitra, J. Nucl. Mater. 297 (2001) 341.
[17] L. Lutterotti, P. Scardi, J. Appl. Crystallogr. 23 (1990) 246.
[18] J.P. Biersack, L.G. Haggmark, Nucl. Instrum. Meth. 174 (1980) 257, The Stopping and Range of Ions in Matter (SRIM 2000) software developed by J. Ziegler and J.P. Biersack is available on the Website http://www.research.ibm.com/ionbeams.
[19] X. Meng, D.O. Northwood, in: ASTM STP, vol. 1023, 1989, p. 478.
[20] A. March, Z. Kristallogr 81 (1932) 285.
[21] W.A. Dollase, J. Appl. Crystallogr. 19 (1986) 267.
[22] G. Will, M. Bellotto, W. Parrish, M. Hatr, J. Appl. Crystallogr. 21 (1988) 182.
[23] E. Tenckhoff, in: Zirconium in the Nuclear Industry, ASTM STP, vol. 754, 1982, p. 5.
[24] G.K. Williamson, R.E. Smallman, Philos. Mag. 1 (1956) 34.
[25] B.E. Warren, in: X-ray Diffraction, Addision-Wesley, Reading, MA, 1969, p. 251.
[26] R.W. Weeks et al., J. Nucl. Mater. 36 (1970) 223.
[27] M. Kiritani, J. Nucl. Mater. 216 (1994) 220.
[28] S.K. Chatterjee, S.K. Halder, S.P. Sengupta, J. Appl. Phys. 47 (1976) 411.
[29] S.K. Chatterjee, S.P. Sengupta, J. Mater. Sci. 9 (1974) 953.
[30] R. Sen, S.K. Chattopadhyay, S.K. Chatterjee, Jpn. J. Appl. Phys. 36 (1997) 364.
[31] R. Sen, S.K. Chattopadhyay, S.K. Chatterjee, Met. Mater. Trans. 29A (1998) 2639.
[32] P. Mukherjee, P. Sen, P. Barat, S.K. Bandyopadhyay, S.K. Chattopadhyay, S.K. Chatterjee, M.K. Mitra, Met. Mater. Trans. 31A (2000) 2405.